


# A closed-loop optogenetic screen for neurons controlling feeding in *Drosophila*

Celia K. S. Lau, Meghan Jelen, and Michael D. Gordon \*

Department of Zoology and Life Sciences Institute, University of British Columbia, Vancouver, BC V6T 1Z3, Canada

\*Corresponding author: gordon@zoology.ubc.ca

## Abstract

Feeding is an essential part of animal life that is greatly impacted by the sense of taste. Although the characterization of taste-detection at the periphery has been extensive, higher order taste and feeding circuits are still being elucidated. Here, we use an automated closed-loop optogenetic activation screen to detect novel taste and feeding neurons in *Drosophila melanogaster*. Out of 122 Janelia FlyLight Project GAL4 lines preselected based on expression pattern, we identify six lines that acutely promote feeding and 35 lines that inhibit it. As proof of principle, we follow up on *R70C07-GAL4*, which labels neurons that strongly inhibit feeding. Using split-GAL4 lines to isolate subsets of the *R70C07-GAL4* population, we find both appetitive and aversive neurons. Furthermore, we show that *R70C07-GAL4* labels putative second-order taste interneurons that contact both sweet and bitter sensory neurons. These results serve as a resource for further functional dissection of fly feeding circuits.

**Keywords:** Optogenetics; neural activation screen; taste; feeding; *Drosophila*

## Introduction

Gustation is a primary sense conserved across the animal kingdom. It contributes to individual fitness, allowing animals to assess and distinguish between potentially nutritious foods and those that may be toxic. Sweetness, an indicator of energy, generally promotes consumption, whereas bitterness, an indicator of potential toxicity, triggers rejection behavior (Yarmolinsky et al. 2009). However, the details of how gustatory information is relayed through the brain to evoke these corresponding behaviors remains unclear. On-going research efforts in this area are fueled by studies conducted in *Drosophila melanogaster*, owing to the reliability of their innate feeding behaviors and the accessibility of powerful genetic tools.

Similar to mammalian taste receptor cells, fruit flies have gustatory receptor neurons (GRNs) that are capable of detecting basic taste qualities, including sweet, bitter, salt, and acids, responsible for triggering food acceptance or rejection (Scott 2018; Chen and Dahanukar 2020). The tuning of sweet and bitter GRNs is partially dictated by expression of gustatory receptors (GRs). Specifically, Gr5a-positive neurons respond broadly to sweetness and those expressing Gr66a respond to bitter (Thorne et al. 2004; Wang et al. 2004; Marella et al. 2006; Dahanukar et al. 2007). GRNs send projections to the brain, with arborizations terminating in the subesophageal zone (SEZ). This area of the brain is referred to as the primary taste center, acting as the first point of taste signal processing and relay (Rajashankar and Singh 1994; Thorne et al. 2004; Wang et al. 2004; Ito et al. 2014). GRN projection patterns in the SEZ are roughly localized based on the taste modality encoded and the origin of the GRN—from the pharynx, proboscis or legs (Wang et al. 2004; Kwon et al. 2014).

While GRNs are well characterized, only a handful of studies have identified downstream neurons. These include several populations receiving input from sweet GRNs: sweet gustatory projection neurons (sGPNs), which make contact with Gr5a GRNs, project to the antennal mechanosensory and motor center (AMMC), and evoke proboscis extension (Kain and Dahanukar 2015); gustatory second-order neurons (G2N-1s), which also receive synaptic input from Gr5a GRNs, but unlike sGPNs, arborize locally and terminate within the ventral SEZ (Miyazaki et al. 2015); and ingestion neurons (IN1), which are specific to pharyngeal sweet inputs and sufficient to prolong ingestion (Yapici et al. 2016). More recently, a single pair of bilaterally symmetrical interneurons called bitter gustatory local neurons (bGLNs) were shown to be stimulated by bitter tastants and sufficient to inhibit appetitive behavior upon activation (Bohra et al. 2018). Additionally, long-range taste projection neurons (TPNs) relay taste input to regions of the higher brain (Kim et al. 2017). The discovery of these various second-order taste neurons brings us closer to understanding the pathways by which peripheral taste can be translated to behavior. However, a global picture of taste processing in higher order circuits remains obscure, suggesting the need for identifying additional higher order taste and feeding neurons.

Recently, we developed the Sip-Triggered Optogenetic Behavior Enclosure (STROBE) for closed-loop optogenetic activation of neurons during fly feeding (Jaeger et al. 2018; Musso et al. 2019). The STROBE temporally couples LED activation to interactions between a fly and one of two food sources in a small arena. In combination with targeted expression of light-gated cation channels, this system effectively activates peripheral and central

Received: August 20, 2020. Accepted: March 03, 2021

© The Author(s) 2021. Published by Oxford University Press on behalf of Genetics Society of America.

This is an Open Access article distributed under the terms of the Creative Commons Attribution License (<http://creativecommons.org/licenses/by/4.0/>), which permits unrestricted reuse, distribution, and reproduction in any medium, provided the original work is properly cited.

neurons, allowing real-time modulation of the fly's sensory experience or motor patterns during feeding (Musso *et al.* 2019). The preference of the fly for the light-triggering food compared to the nonlight-triggering food indicates the appetitive, aversive, or neutral valence of the neurons undergoing optogenetic activation.

In this study, 122 *Janelia FlyLight* Project enhancer-GAL4 lines (Jenett *et al.* 2012) were crossed with *UAS-CsChrimson* and subjected to testing in the STROBE. We found six lines that produced a preference for the light-triggering food and 35 lines that drove preference for the nonlight-triggering food. One line in particular, *R70C07-GAL4*, was chosen for further characterization of its role in feeding inhibition. A GAL4 hemidriver version of *R70C07* (*R70C07-p65*) was combined with five different GAL4.DBD hemidrivers to generate five split-GAL4s labeling subsets of a SEZ interneuron population that is prominent within the *R70C07-GAL4* expression pattern. Unexpectedly, while one split-GAL4 line phenocopied the aversion seen with *R70C07-GAL4* activation, another drove the opposite effect (attraction), and three produced small or insignificant effects. GFP reconstitution across synaptic partners (GRASP) revealed that neurons within the identified SEZ interneuron population make contact with both sweet and bitter GRNs, suggesting a role in taste processing. The results presented here demonstrate the feasibility of using the STROBE to identify novel candidate taste and feeding neurons, and provide a resource of lines for further investigation in the future.

## Materials and methods

### Drosophila stocks and crosses

Fly stocks were raised on standard cornmeal-dextrose fly food at 25°C in 70% humidity. *20XUAS-IVS-CsChrimson.mVenus* (BDSC, stock number: 55135) was used for optogenetic activation. See S1 for the full list of enhancer-GAL4 lines of the *Janelia FlyLight* Project (<http://flweb.janelia.org/>) that were used for the optogenetic activation screen. The following split-GAL4 lines were created by combining selected hemidrivers with *R70C07-p65.AD* (stock 71122): *SEZ1-GAL4* (*R37H08-GAL4.DBD* stock 68786); *SEZ2-GAL4* (*R53C05-GAL4.DBD* stock 69451); *SEZ3-GAL4* (*VT044519-GAL4.DBD* stock 75123); *SEZ4-GAL4* (*R38E08-GAL4.DBD* stock 69427); and *SEZ5-GAL4* (*R10E08-GAL4.DBD* stock 69792). For GRASP experiments we used: *Gr5a-LexA::VP16*, *UAS-CD4::spGFP1-10*, *LexAop-CD4::spGFP11*, *UAS-CD8::dsRed* (Gordon and Scott 2009) and *Gr66a-LexA::VP16* (Thistle *et al.* 2012).

### Fly preparation and STROBE experiments

Flies were maintained at 25°C in 70% humidity. Females (2–5 d after eclosion) were collected and allowed to recover in fresh vials containing standard medium for at least 1 d before being transferred to covered vials that contained 1 ml standard medium with either 1 mM of all-*trans*-retinal and 1% ethanol as a vehicle (retinal-fed group) or ethanol vehicle alone (nonretinal-fed controls) for 2 days. Flies were then starved for 20–24 hours in similar conditions, except the standard medium was replaced with 1% agar. As such, flies were maintained on either + or - all-*trans*-retinal diets throughout the 3 days that preceded testing. To promote food interaction during testing, flies were water-deprived for 1 hour.

Both channels of the STROBE chambers were loaded with 4  $\mu$ l of 1% agar for the activation screen. Some follow-up experiments were performed with 100 mM sucrose in 1% agar to further promote food interactions. To commence each experiment, the acquisition on the STROBE software was initiated before flies were individually placed in each arena via mouth aspiration.

Experiments were 1 hour in duration and the preference indices were calculated as: (Interactions with Food 1—Interactions with Food 2)/(Interactions with Food 1 + Interactions with Food 2). The red LED is always associated to the left channel, with Food 1. Details of the STROBE system, including the design and programming were previously described (Musso *et al.* 2019).

### Optogenetic geotaxis assay

Female flies were collected in groups of 10 per vial, 2–5 days post eclosion and maintained at 25°C in 70% humidity. Flies were placed on either 1 mM all-*trans*-retinal supplemented food, or vehicle control food for 3 days prior to the assay. One hour before the assay, flies were transferred into empty vials. The assay was performed as described in (Stafford *et al.* 2012). Flies were tapped to the bottom of the vial as a red LED light was turned on. Flies were allowed to freely climb, and the number of flies to reach a height of 7.5 cm after a total of 8 seconds was recorded. For each group, the assay was repeated a total of 4 times. The climbing index was calculated as an average per vial, and across 4 independent groups of the same genotype.

### Immunohistochemistry

Brain immunohistochemistry was performed as previously described (Chu *et al.* 2014). To stain flies with the *UAS-CsChrimson.mVenus* transgene, the following primary antibodies were used: mouse anti-brp (1:50, Developmental Studies Hybridoma Bank #nc82) and rabbit anti-GFP (1:1000, Invitrogen), with secondary antibodies: goat anti-rabbit Alexa-488 (A11008, Invitrogen) and goat anti-mouse Alexa-546 (A11030, Invitrogen). For GRASP experiments, the following were used as primary antibodies: mouse anti-GFP (1:100, Sigma-Aldrich, G6539), rat anti-DN-cadherin (1:25, DSHB DNEX#8), and rabbit anti-DsRed (1:1000, Clontech #632496) with secondary antibodies: goat anti-mouse Alexa-488 (A11029, Invitrogen), goat anti-rat Alexa-568 (A11077, Invitrogen) and goat anti-rabbit Alexa-647 (A21245, Invitrogen).

All images were acquired using a Leica SP5 II Confocal microscope. Images taken at a magnification of 25x were with a water immersion objective with a Z-stack step size of 1  $\mu$ m, while those imaged at 63x were with oil immersion and a step size of 0.5  $\mu$ m.

### Statistics and data exclusion

The STROBE sometimes records very small or very large interaction numbers due to technical malfunctions. To account for this, trials from individual flies were removed under three conditions: (i) if no interactions were recorded from the light-triggering channel; (ii) if fewer than five interactions were recorded on the non-light-triggering channel; (iii) if the number of interactions was more than 2.68 standard deviations from the mean. The rationale for (i) and (ii) is that very aversive neurons can produce few interactions on the light-triggering channel, but flies will generally record more than five interactions on the other channel in a functional trial.

Statistical tests were performed using Graphpad Prism 6. T-tests were used to compare experimental (retinal fed) to control (same genotype not fed retinal). The purpose of these statistics is to evaluate the significance of effects within individual genotypes for the purposes of selecting lines for follow-up, rather than to minimize the overall false positive rate. Therefore, no correction was applied when combining the different genotypes in the summary graph shown in Figure 1.

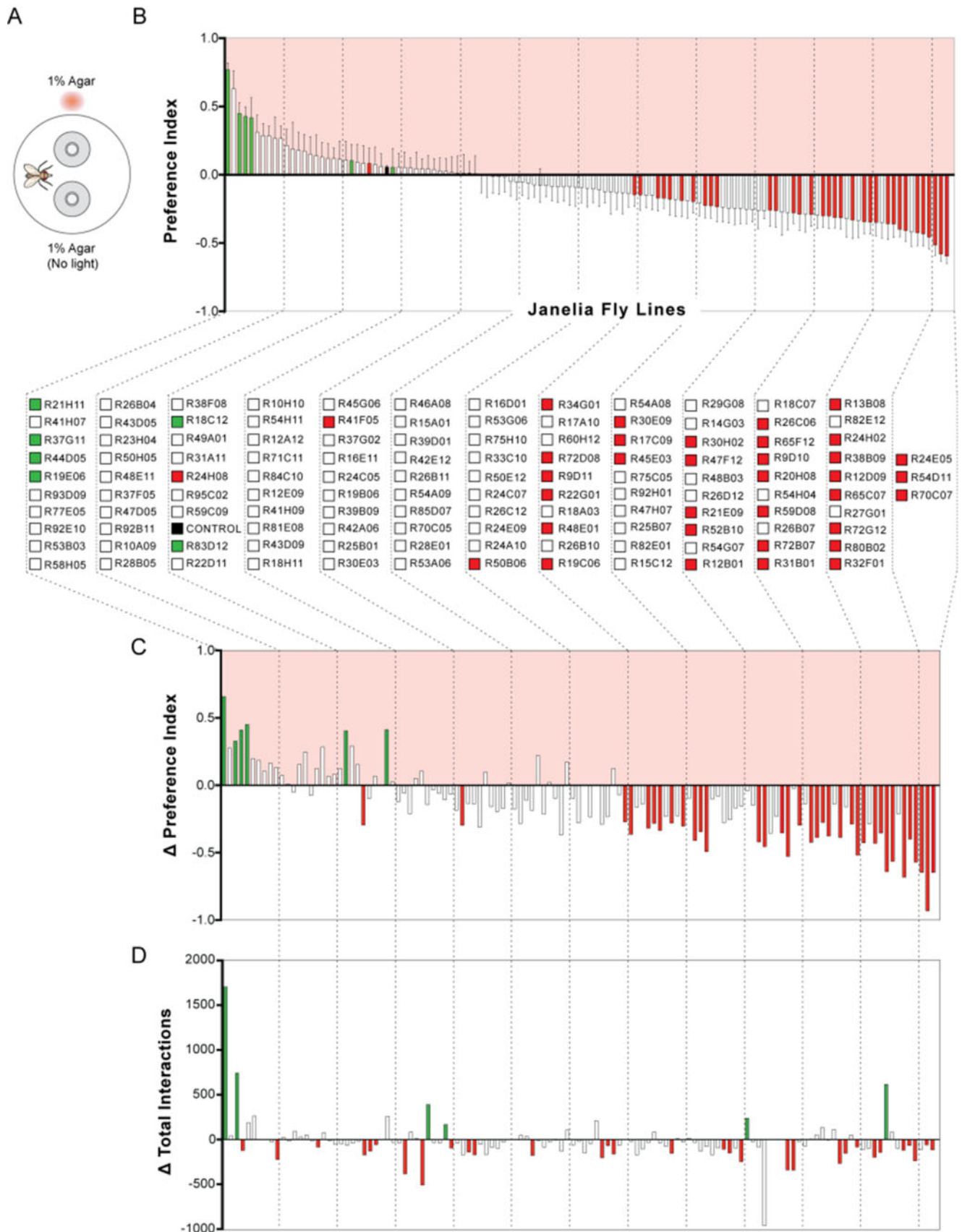


**Figure 1** Summary of STROBE screen results. (A) Experimental setup: each STROBE arena contains two channels containing 1% agar, and only interactions with one of the channels triggers red light activation. (B) Mean preference indices of GAL4 driver lines that were tested in the STROBE. A positive PI indicates preference for the light-triggering food, while a negative PI indicates avoidance of the light-triggering food. Color code indicates significance compared to genetically identical, nonretinal-fed controls (control preferences for each line not shown): green bars denote significantly

## Data availability

All raw numerical data are available for download from figshare: <https://doi.org/10.25387/g3.14160920>. Reagents are available upon request.

## Results and discussion

### Optogenetic screening of driver lines with the STROBE

The *Janelia FlyLight* Project has generated more than 8000 transgenic GAL4 lines, providing a vast resource for manipulating specific neurons in the fly brain (Pfeiffer *et al.* 2008; Jenett *et al.* 2012). We selected 122 GAL4 driver lines from the collection based on the criteria that each selected line must sparsely label neurons that have not yet been implicated in taste and have split-GAL4 versions available for use. Importantly, these parameters predetermine the feasibility of further neural population refinement since sparseness allows for the systematic selection of different neuron populations to isolate via split-GAL4 combinations. Flies expressing *CsChrimson* under control of the selected GAL4 drivers were fed all-*trans*-retinal, a cofactor required for channel function, three days prior to the experiment, whereas control flies of the same genotype were not fed all-*trans*-retinal. Flies were individually mouth-aspirated into STROBE arenas containing two choices of identical plain agar (1%), where interactions with one of the choices triggers a red LED light to excite neurons expressing functional *CsChrimson* (Figure 1A). Flies that choose both options equally would have a near-zero preference index (PI), while flies that interacted relatively more or less with the light-paired option are represented by positive and negative PIs, respectively.

Our screen identified six GAL4 lines that produced a significantly positive preference in the STROBE compared to their matched isogenetic no-retinal controls, and 35 lines that produced a significantly negative preference (Figure 1B). Because food interactions measured in the STROBE correlate with food consumption (Itskov *et al.* 2014; Musso *et al.* 2019), we can interpret these lines as containing neurons that acutely impact feeding behavior. Notably, there are examples where a significant difference from controls was observed, despite an absolute preference near zero. This is because each line was compared to its own set of controls, and there are cases where the control group displayed a preference that deviated from neutrality, despite the fact that pooling all the controls revealed the expected preference near zero (Figure 1B). The difference between experimental and control preferences for each line is displayed in Figure 1C. We also identified lines that produced a change in total sip number across both food choices, which may or may not be associated with a change in preference (Figure 1D). These lines could contain neurons exerting persistent modulation of feeding that lasts beyond the time period of individual feeding events, and therefore affects interactions with both the light-triggering and nonlight-triggering food options. Detailed data for each line, including expression, time curves and interaction numbers for each replicate is presented in graphical form (Supplementary File S1) and raw data is available for

download (Supplementary Files S2 and S3) in the Supplementary materials.

By pitting the choice of agar against agar paired with neuronal activation, we were able to efficiently identify driver lines labeling neurons that impact feeding in either a positive or negative direction. One question is why we observed more lines producing a negative feeding preference. We speculate that this is because there are many ways to decrease feeding, such as paralysis, inducing a behavior that interrupts feeding, or producing any kind of negative percept. On the other hand, we expect effects that increase feeding to be relatively more specific to taste or feeding.

### Subsets of the R70C07-GAL4 neuron population drive opposing feeding behaviors

We identified R70C07-GAL4 to be a driver line of interest, as it showed the strongest feeding aversion upon neuronal activation (Figure 1B). Immunofluorescence of brains and ventral nerve cords (VNCs) from R70C07-GAL4>*CsChrimson* flies revealed a prominent set of 15 strongly labelled cell bodies on each side of the SEZ, with dense arborization across the medial and lateral SEZ (Figure 2A). Weaker and sparser projections were also observed in the antennal lobes and superior medial protocerebrum. Despite the absence of labellar and pharyngeal taste projections in this driver, stereotypical leg GRN projections were observed in the SEZ, as well as weak VNC processes, which could be contributing to the aversive feeding behavior observed in the STROBE (Stocker 1994). We retested R70C07>*CsChrimson* flies in the STROBE with the addition of 100mM sucrose to both 1% agar options, which we have previously shown to enhance negative effects by increasing overall interaction numbers (Musso *et al.* 2019). This revealed intense aversion to the light-triggering side reminiscent of bitter GRN activation in the STROBE (Figure 2, B and C; Jaeger *et al.* 2018; Musso *et al.* 2019).

To identify the specific neurons involved in feeding aversion, split-GAL4 lines (Luan *et al.*; Tirian and Dickson 2017; Dionne *et al.* 2018) were created by combining the R70C07-*p65.AD* hemidriver with various GAL4 DNA binding domain (DBD) hemidrivers selected based on putative expression in the SEZ neuron population (Figures 2 and 3). Leg projections and most VNC projections were successfully eliminated in R70C07-*p65.AD*; R37H08-GAL4.DBD (combination called SEZ1-GAL4) and R70C07-*p65.AD*; R53C05-GAL4.DBD (SEZ2-GAL4) (Figure 2, D and G). Additionally, this intersectional refinement reduced the number of SEZ neurons from 15 per side in the original R70C07-GAL4 driver to subsets of 3 and 7 in SEZ1-GAL4 and SEZ2-GAL4, respectively. Light-activation of SEZ1>*CsChrimson* flies in the STROBE inhibited feeding similar to R70C07-GAL4 (Figure 2, E and F). The effect magnitude was slightly reduced, which could be explained by the elimination of either the leg inputs or subsets of SEZ neurons. Surprisingly, light-activation of SEZ2-GAL4 produced the opposite effect by strongly promoting feeding (Figure 2, H and I). We also identified three additional split-GAL4 combinations that had small or no significant effect on feeding. SEZ3-GAL4 labels 7 neurons per side of the SEZ and produced mild but significant feeding

more positive preference than controls and red bars denote lines that generated a significantly more negative preference than controls; the dark gray bar shows the aggregate responses of the nonretinal controls across all experiments. Values represent mean  $\pm$  SEM.  $n = 9-35$ , except for the aggregate control where  $n = 1978$  (this aggregate control was not used for any statistical testing). (C) Difference in PI between experimental and control groups for each line. Bars are color coded as in (B). (D) Difference in average total interaction numbers across both channels (light and nonlight) for each line. Color code indicates significance compared to nonretinal controls for each line: green bars denote significantly elevated interactions compared to controls; red bars indicate significantly suppressed interactions compared to controls. Detailed results for all lines are depicted graphically in Supplementary File S1 and raw data are presented in Supplementary Files S2 and S3.

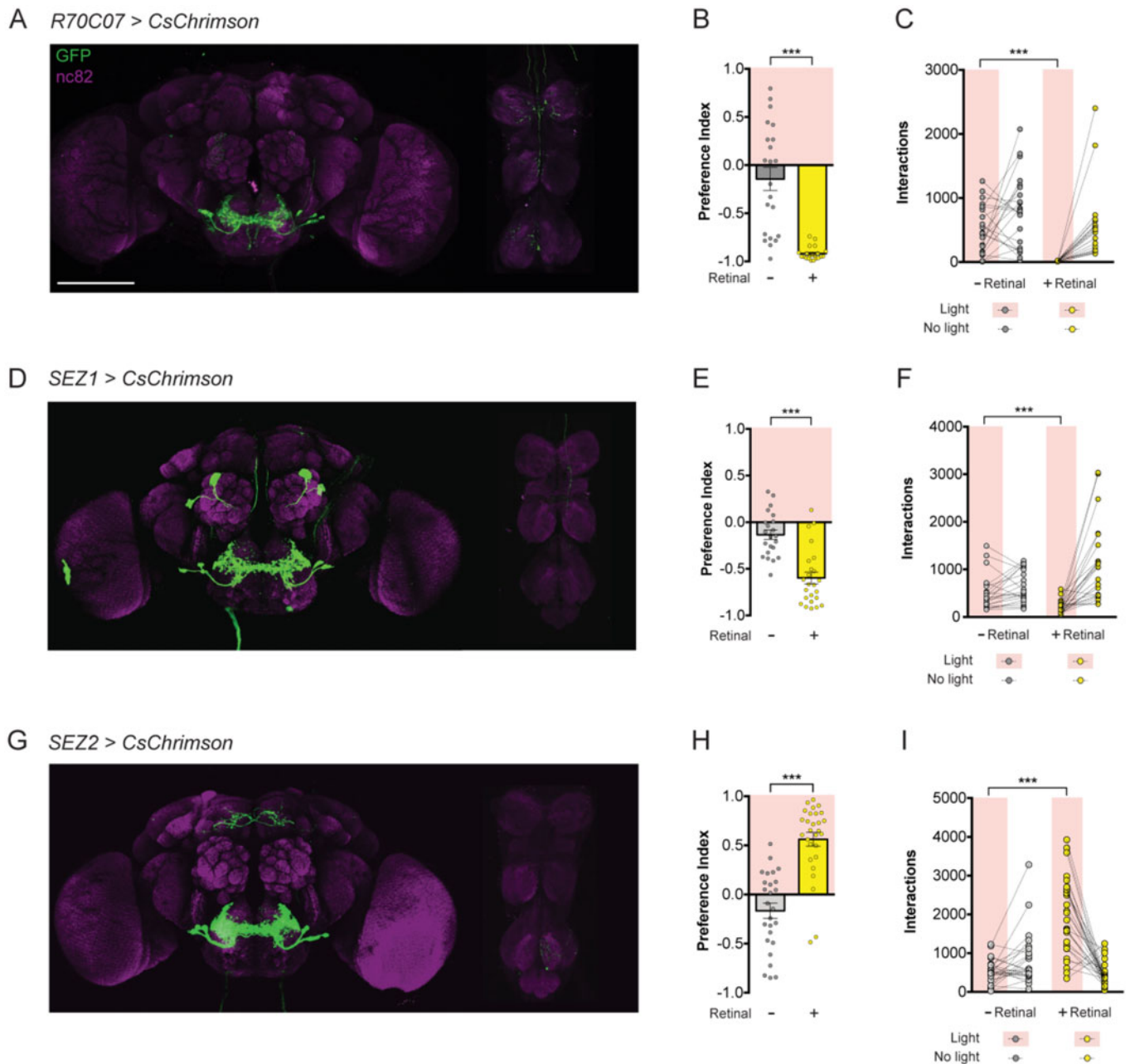


**Figure 2** Subsets of the *R70C07-GAL4* population drive opposing feeding behaviors. (A–C) *R70C07-GAL4, UAS-CsChrimson.mVenus* expression in the brain and VNC (A), PI in the STROBE containing 100 mM sucrose in 1% agar in both channels (B), and individual interaction numbers from the same experiment (C). (D–F) *SEZ1-GAL4* expression (D), PI in the STROBE containing 100 mM sucrose in 1% agar in both channels (E), and interaction numbers (F). (G–I) *SEZ2-GAL4* expression (G), PI in the STROBE containing 100 mM sucrose in 1% agar in both channels (H), and interaction numbers (I). For immunofluorescence (A, D, and G) brains and VNC are stained for GFP (green) and nc82 (magenta). Scale bars, 100  $\mu$ m. For preference indices (B, E, and H), yellow bars represent the retinal fed group and gray bars represent the no-retinal controls of the same genotype. Values are mean  $\pm$  SEM. For individual interaction numbers (C, F, and I), lines connect values for individual flies.  $n = 21$ –28. Statistical tests: t-test, \*\*\* $P < 0.001$ . Raw data are available in Supplementary File S4.

inhibition compared to controls (Figure 3, A–C). *SEZ4-GAL4* and *SEZ5-GAL4* label 2–3 and 4–5 neurons per side, respectively, but produced no significant behavioral effect in the STROBE, although both trended in the negative direction (Figure 3, D–I).

There are two possible broad explanations for the phenotypes observed following split-GAL4 refinement. First, it is possible that the *R70C07* SEZ population comprises multiple neuron types with different behavioral effects. Perhaps *SEZ1-GAL4* isolated a predominantly negative set, while *SEZ2-GAL4* isolated a subset that was predominantly positive. This theory can be extended to suggest that the

three split-GAL4 lines producing little or no effect labeled both positive and negative SEZ neurons that effectively cancelled each other out. The second possibility is that neurons outside the SEZ population affected preference in one or more of the split-GAL4 populations. Notably, both *SEZ1-GAL4* and *SEZ2-GAL4* labeled 1–2 neurons that were not clearly visible in the original *R70C07* driver. These could reflect differences in expression between *R70C07-GAL4* and *R70C07-p65.AD*, and may have an impact on behavior.

Although the bidirectional modulation of feeding suggests a specific role for the identified SEZ neurons in feeding

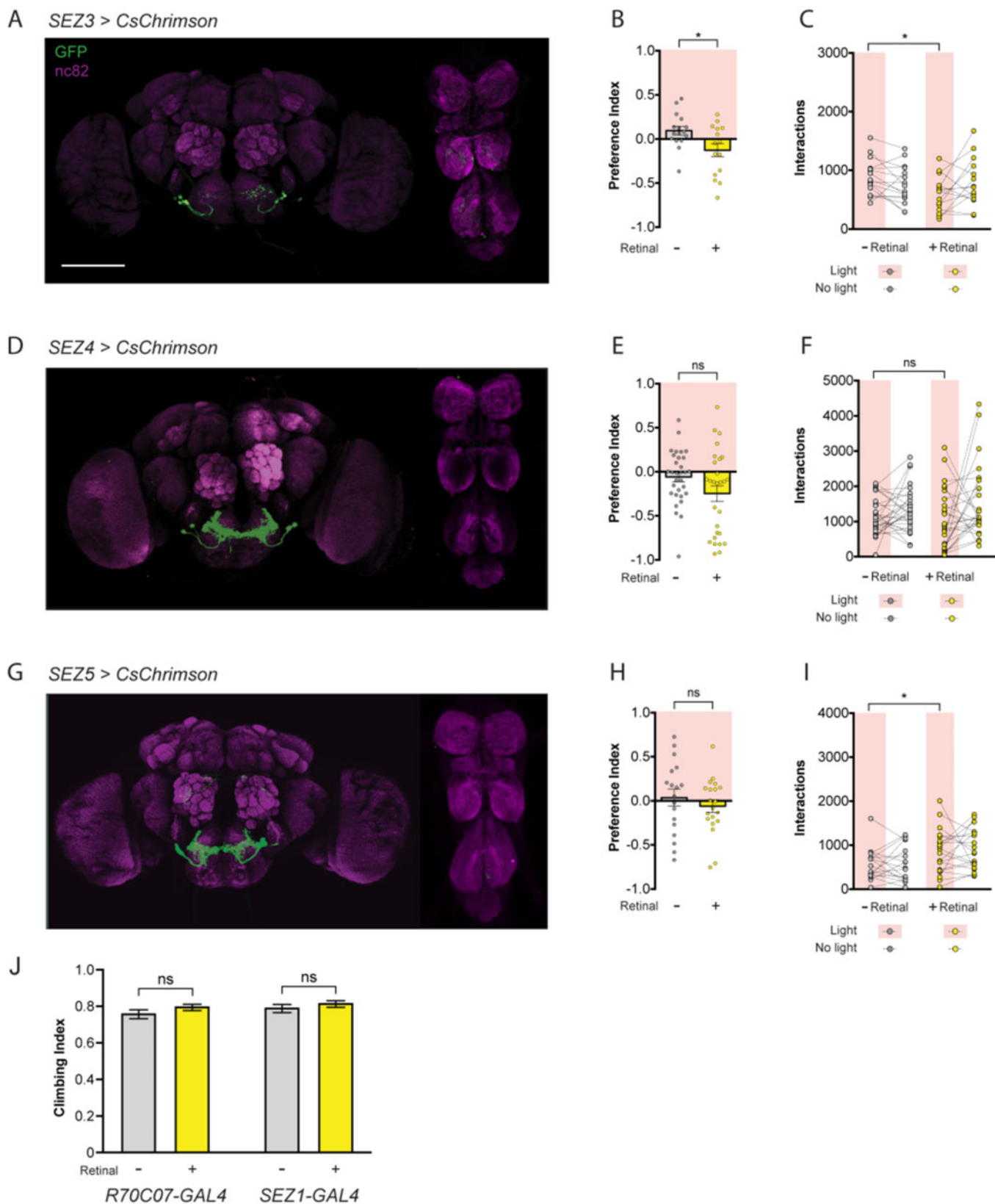


**Figure 3** Not all *R70C07-GAL4* *SEZ* neurons are sufficient to alter feeding. (A–C) *SEZ3-GAL4* expression in the brain and VNC (A), PI in the STROBE containing 100 mM sucrose in 1% agar in both channels (B), and individual interaction numbers from the same experiment (C). (D–F) *SEZ4-GAL4* expression (D), PI in the STROBE containing 100 mM sucrose in 1% agar in both channels (E), and interaction numbers (F). (G–I) *SEZ5-GAL4* expression (G), PI in the STROBE containing 100 mM sucrose in 1% agar in both channels (H), and interaction numbers (I). For immunofluorescence (A, D, G) brains and VNC are stained for GFP (green) and nc82 (magenta). Scale bars, 100  $\mu$ m. For preference indices (B, E, and H), yellow bars represent the retinal fed group and gray bars represent the no-retinal controls of the same genotype. Values are mean  $\pm$  SEM. For individual interaction numbers (C, F, and I), lines connect values for individual flies.  $n = 15$ –31. (J) Climbing indices of *R70C07-GAL4* and *SEZ1-GAL4* crossed to *UAS-CsChrimson* and activated with red light, compared to controls without retinal.  $n = 16$  tests per genotype. Statistical tests: t-test, \* $P < 0.05$ , ns = not significant. Raw data are available in Supplementary File S4.

regulation, we also considered the possibility that the *R70C07-GAL4* and *SEZ1-GAL4* populations produce behavioral effects that indirectly impact feeding, for example through changes in mobility. To test whether either line had a gross effect on locomotion we subjected each to a climbing assay while being activated with the same LED present in the STROBE. Neither line produced a measurable change compared to controls, consistent with each imposing a direct effect on feeding behavior (Figure 3J). In the future, additional split-GAL4 lines that completely eliminate all expression outside the SEZ will be required to tease apart the exact roles of the SEZ subsets present in *R70C07-GAL4*.

## Two distinct neuronal clusters make up the *R70C07* SEZ population

Closer examination of *R70C07-GAL4* revealed that the SEZ cluster is actually composed of two distinct clusters. Cluster 1 is comprised of eight neurons on each side that arborize medially and laterally within the SEZ. Cluster 2 is comprised of seven neurons with more anterior cell bodies and processes that project close to the antennal nerve into the posterior SEZ, where the arbors remain mostly lateral (Figure 4A). *SEZ1-*, *SEZ2-*, *SEZ4-*, and *SEZ5-GAL4* all label neurons from cluster 1, while *SEZ3-GAL4* labels all seven of the neurons in cluster 2 (Figure 4, B–D). Based on the mild phenotype from *SEZ3-GAL4* activation we suspect that the

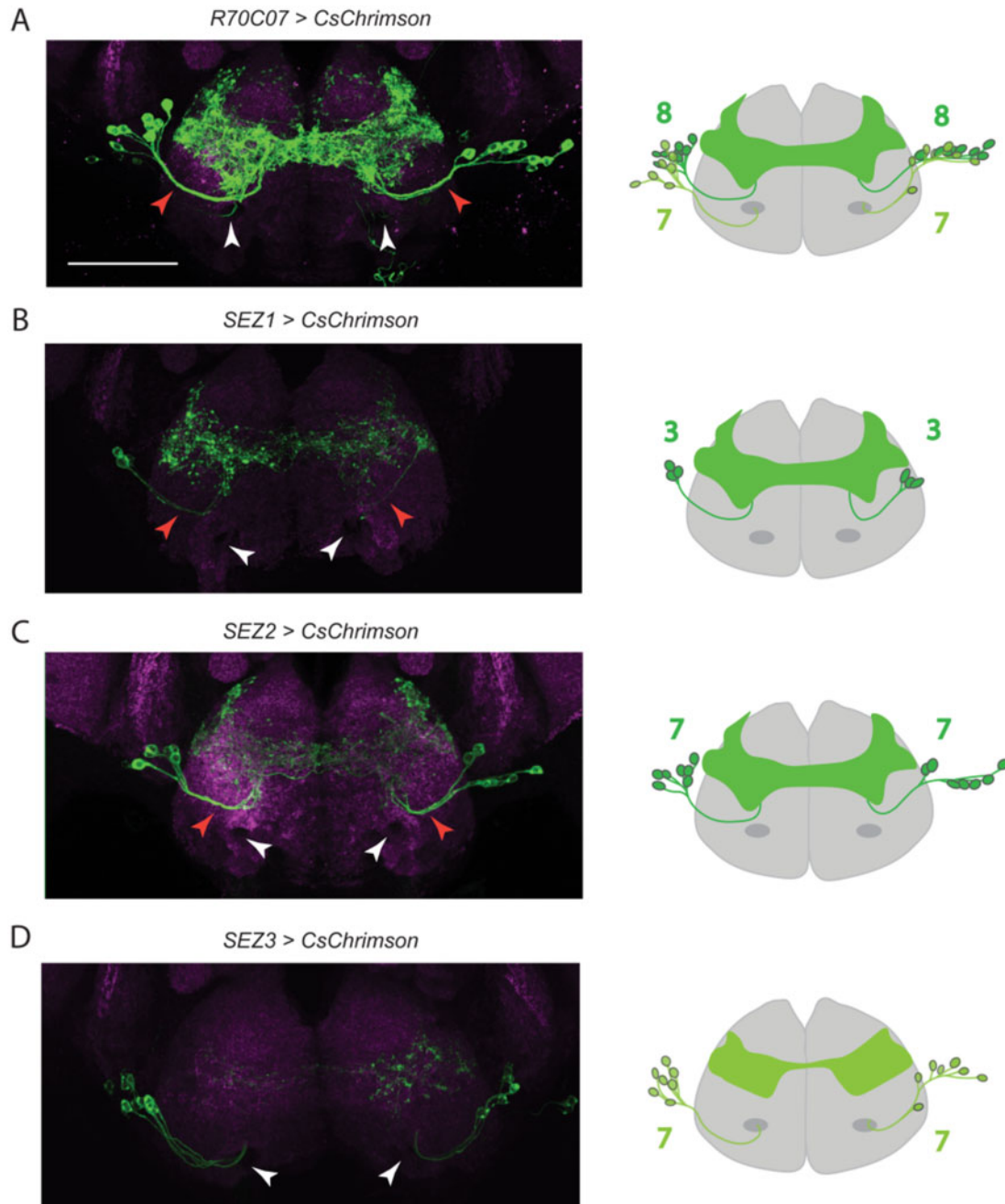


**Figure 4** Two distinct neuronal clusters make up the *R70C07* SEZ population. Immunofluorescent detection of *UAS-CsChrimson.mVenus* (green) driven by *R70C07-GAL4* (A), *SEZ1-GAL4* (B), *SEZ2-GAL4* (C), and *SEZ3-GAL4* (D) in the SEZ with schematics on the right showing the number of neurons labelled by each split-GAL4. *SEZ1-GAL4* and *SEZ2-GAL4* label SEZ neurons that follow the same tract (red arrowhead). *SEZ3-GAL4* labels a distinct group of SEZ neurons that project more ventrally near the labelar nerve tracts (white arrows). Counterstain is *nc82* (magenta). All scale bar is 50  $\mu\text{m}$ .

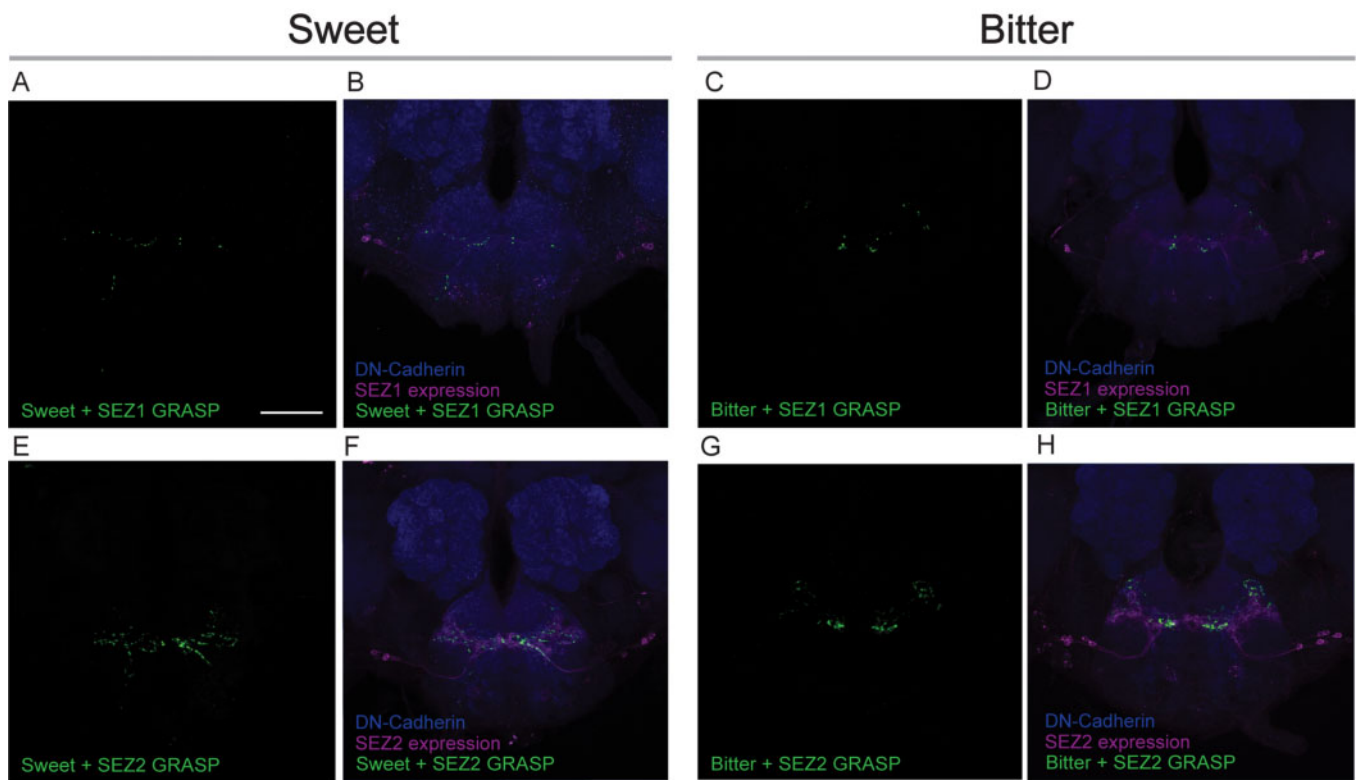


**Figure 5** The SEZ1-GAL4 and SEZ2-GAL4 populations both contact sweet and bitter GRNs. (A–D) GRASP between SEZ1-GAL4 and sweet (A and B) or bitter (C and D) GRNs. (E–H) GRASP between SEZ2-GAL4 and sweet (E and F) or bitter (G and H) GRNs. Antibodies: anti-DN-Cadherin for counterstain (blue), anti-DsRed for GAL4 expression (magenta), anti-GFP used for GRASP signal (green). Scale bar is 50  $\mu$ m.

neurons in cluster 2 are not the primary drivers of *R70C07*-mediated feeding inhibition. However, we cannot rule out the possibility that lower expression levels in SEZ3-GAL4 also contribute to its lesser effect.

### Bitter and sweet sensory neurons GRASP with lateral SEZ neurons

We next wondered whether insight into the opposing behavioral effects of SEZ1-GAL4 and SEZ2-GAL4 could be gleaned from examining the synaptic inputs to these neurons. Thus, we used GFP-reconstitution across synaptic partners (GRASP) to test for contacts with sweet and bitter GRNs. One half of the split-GFP reporter (*lexAop-spGFP11*) was targeted to either the bitter- or sweet-sensitive GRNs using *Gr66a-LexA* or *Gr5a-LexA* as a driver; and the other half of the split-GFP reporter (*UAS-spGFP1-10*) was targeted to the lateral SEZ neurons with either SEZ1- (Figure 5, A–D) or SEZ2-GAL4 (Figure 5, E–H). Unexpectedly, bitter and sweet GRASP signals were detected for both split-GAL4 lines, suggesting that bitter and sweet GRNs interact with at least one of the neurons labelled by each line. Because our behavioral data suggests the possibility of two types of neurons with opposing valence within *R70C07*-GAL4 SEZ population, one possible interpretation of the GRASP results is that each of those populations receives input from either sweet or bitter GRNs. Alternatively, one or more neurons within the population could synapse with both sweet and bitter GRNs, perhaps playing a role in taste integration such as inhibitory feedback (Chu et al. 2014). Notably, since *Gr5a* is not expressed in the pharyngeal sense organs, the strong GRASP signal with *Gr5a* GRNs suggests an interaction with inputs from the labellum. This emphasizes the distinction between *R70C07*-GAL4 SEZ neurons and the previously characterized and

morphologically similar IN1 neurons, which receive sweet input from the pharyngeal sense organs and are negative for GRASP with *Gr5a* GRNs (Yapici et al. 2016). Further analysis with calcium imaging will be necessary to determine the functional interactions between GRNs and the *R70C07*-GAL4 SEZ neurons.

Although the evidence that the *R70C07* SEZ population represents bona fide second-order taste neurons is incomplete, neurons that appear very similar were previously identified as postsynaptic to sweet GRNs using the trans-synaptic tracer trans-Tango (Talay et al. 2017). The split-GAL4 lines identified in our study should greatly aid in more fully characterizing the functional properties of these neurons, including their inputs and post-synaptic targets. We also anticipate that the other lines identified in our behavioral screen will serve as useful starting points in the long-term prospect of more fully understanding the neural control of feeding behavior in flies.

### Acknowledgments

We thank Pierre Junca and Pierre-Yves Musso for help in identifying split-GAL4 hemidriviers, and members of the Gordon lab for comments on the manuscript. We also thank the Bloomington stock center for flies and the Janelia Flylight project for generating the lines screened and for the expression patterns shown in Supplementary File S1.

### Funding

This work was funded by the Canadian Institutes of Health Research (CIHR) operating grant FDN-148424, with infrastructure funded by the Canadian Foundation for Innovation (CFI) grant



27290. M.D.G. is a Michael Smith Foundation for Health Research Scholar.

**Conflicts of interest:** We have no conflicts of interest to declare.

## Literature cited

- Bohra AA, Kallman BR, Reichert H, VijayRaghavan K. 2018. Identification of a single pair of interneurons for bitter taste processing in the *Drosophila* brain. *Curr Biol*. 28:847–858.e3.
- Chen Y-CD, Dahanukar A. 2020. Recent advances in the genetic basis of taste detection in *Drosophila*. *Cell Mol Life Sci*. 77:1087–1101.
- Chu B, Chui V, Mann K, Gordon MD. 2014. Presynaptic gain control drives sweet and bitter taste integration in *Drosophila*. *Curr Biol*. 24:1978–1984.
- Dahanukar A, Lei Y-T, Kwon JY, Carlson JR. 2007. Two Gr genes underlie sugar reception in *Drosophila*. *Neuron* 56:503–516.
- Dionne H, Hibbard KL, Cavallaro A, Kao J-C, Rubin GM. 2018. Genetic reagents for making split-GAL4 lines in *Drosophila*. *Genetics* 209:31–35.
- Gordon MD, Scott K. 2009. Motor control in a *Drosophila* taste circuit. *Neuron* 61:373–384.
- Ito K, Shinomiya K, Ito M, Armstrong JD, Boyan G, et al. 2014. A systematic nomenclature for the insect brain. *Neuron* 81:755–765.
- Itskov PM, Moreira J-M, Vinnik E, Lopes G, Safarik S, et al. 2014. Automated monitoring and quantitative analysis of feeding behaviour in *Drosophila*. *Nat Commun*. 5:4560.
- Jaeger AH, Stanley M, Weiss ZF, Musso P-Y, Chan RC, et al. 2018. A complex peripheral code for salt taste in *Drosophila*. *eLife* 7:e37167.
- Jenett A, Rubin GM, Ngo T-TB, Shepherd D, Murphy C, et al. 2012. A GAL4-driver line resource for *Drosophila* neurobiology. *Cell Rep*. 2:991–1001.
- Kain P, Dahanukar A. 2015. Secondary taste neurons that convey sweet taste and starvation in the *Drosophila* brain. *Neuron* 85:819–832.
- Kim H, Kirkhart C, Scott K. 2017. Long-range projection neurons in the taste circuit of *Drosophila*. *eLife* 6:e23386.
- Kwon JY, Dahanukar A, Weiss LA, Carlson JR. 2014. A map of taste neuron projections in the *Drosophila* CNS. *J Biosci*. 39:565–574.
- Luan H, Peabody NC, Vinson CR, White BH. 2006. Refined Spatial Manipulation of Neuronal Function by Combinatorial Restriction of Transgene Expression. *Neuron* 52:425–436.
- Marella S, Fischler W, Kong P, Asgarian S, Rueckert E, et al. 2006. Imaging taste responses in the fly brain reveals a functional map of taste category and behavior. *Neuron* 49:285–295.
- Miyazaki T, Lin T-Y, Ito K, Lee C-H, Stopfer M. 2015. A gustatory second-order neuron that connects sucrose-sensitive primary neurons and a distinct region of the gnathal ganglion in the *Drosophila* brain. *J Neurogenet*. 29:144–155.
- Musso P-Y, Junca P, Jelen M, Feldman-Kiss D, Zhang H, et al. 2019. Closed-loop optogenetic activation of peripheral or central neurons modulates feeding in freely moving *Drosophila*. *eLife* 8:e45636.
- Pfeiffer BD, Jenett A, Hammonds AS, Ngo T-TB, Misra S, et al. 2008. Tools for neuroanatomy and neurogenetics in *Drosophila*. *Proc Natl Acad Sci USA*. 105:9715–9720.
- Rajashankar KP, Singh RN. 1994. Neuroarchitecture of the tritocerebrum of *Drosophila melanogaster*. *J Comp Neurol*. 349:633–645.
- Scott K. 2018. Gustatory Processing in *Drosophila melanogaster*. *Annu Rev Entomol*. 63:15–30.
- Stafford JW, Lynd KM, Jung AY, Gordon MD. 2012. Integration of taste and calorie sensing in *Drosophila*. *J Neurosci*. 32:14767–14774.
- Stocker RF. 1994. The organization of the chemosensory system in *Drosophila melanogaster*: a review. *Cell Tissue Res*. 275:3–26.
- Talay M, Richman EB, Snell NJ, Hartmann GG, Fisher JD, et al. 2017. Transsynaptic mapping of second-order taste neurons in flies by trans-tango. *Neuron* 96:783–795.e4.
- Thistle R, Cameron P, Ghorayshi A, Dennison L, Scott K. 2012. Contact chemoreceptors mediate male-male repulsion and male-female attraction during *Drosophila* courtship. *Cell* 149:1140–1151.
- Thorne N, Chromey C, Bray S, Amrein H. 2004. Taste perception and coding in *Drosophila*. *Curr Biol*. 14:1065–1079.
- Tirian L, Dickson BJ. 2017. The VT GAL4, LexA, and split-GAL4 driver line collections for targeted expression in the *Drosophila* nervous system. *bioRxiv*. doi:10.1101/198648.
- Wang Z, Singhvi A, Kong P, Scott K. 2004. Taste representations in the *Drosophila* brain. *Cell* 117:981–991.
- Yapici N, Cohn R, Schusterreiter C, Ruta V, Vosshall LB. 2016. A taste circuit that regulates ingestion by integrating food and hunger signals. *Cell* 165:715–729.
- Yarmolinsky DA, Zuker CS, Ryba NJP. 2009. Common sense about taste: from mammals to insects. *Cell* 139:234–244.

Communicating editor: M. Ramaswami